

## RESONANT INTERACTION BETWEEN LOCAL VIBRATIONAL MODES AND EXTENDED LATTICE PHONONS IN ALSb

M.D. McCluskey<sup>1</sup>, E.E. Haller, W. Walukiewicz, and P. Becla<sup>2</sup>

Lawrence Berkeley National Laboratory, MS 2-200, 1 Cyclotron Rd., Berkeley CA 94720, USA

<sup>1</sup>Present address: Xerox PARC, 3333 Coyote Hill Rd., Palo Alto, CA 94304

<sup>2</sup>Department of Materials Science and Engineering, Massachusetts Institute of Technology, Cambridge, MA 02139

**Keywords:** Local vibrational modes (LVM's), ALSb, DX centers, hydrogen

**Abstract.** Using infrared spectroscopy we have observed Se-H stretch and wag local vibrational modes (LVM's) in ALSb. The frequencies of the wag mode harmonics are explained by perturbation theory. In addition, there is evidence of a resonant interaction between LVM's and multi-phonon modes. This interaction leads to a splitting of the Se-H stretch mode into three peaks at 1606.3, 1608.6, and 1615.7  $\text{cm}^{-1}$  at liquid-helium temperatures. As the temperature or pressure is increased, the stretch mode and multi-phonon modes show anti-crossing behavior.

### Introduction.

In this paper, we report evidence of a resonant interaction between LVM's and extended lattice phonons that gives rise to a new collective excitation called a "localon." This resonance is similar to the Fermi resonance between wag and stretch local vibrational modes (LVM's) in donor-hydrogen complexes in silicon [1]. By varying the temperature and pressure to change the phonon energies, we have studied the evolution of the localon spectra in ALSb.

As we have noted previously [2], at liquid-helium temperatures, hydrogenated ALSb:Se has stretch mode peaks at 1608.6 and 1615.7  $\text{cm}^{-1}$ , whereas the Se-D mode has only one stretch mode peak at 1173.4  $\text{cm}^{-1}$ . In addition, there is a small Se-H peak at 1606.3  $\text{cm}^{-1}$ . Hydrogenated and deuterated ALSb:Te have only one stretch mode peak each, at 1599.0 and 1164.4  $\text{cm}^{-1}$  respectively. The ratio of the three Se-H peak areas is constant from sample to sample, which suggests that they are not due to additional impurity complexes. The details of the crystal growth, sample preparation, and hydrogenation techniques are given in Ref. 2.

### Experimental details.

Variable temperature spectra were obtained with a Bomem DA8 spectrometer with a KBr beamsplitter and a mercury cadmium telluride (MCT) detector. Variable pressure spectra were obtained with a Digilab 80-E spectrometer with a KBr beamsplitter and an instrumental resolution of 1  $\text{cm}^{-1}$ . To generate hydrostatic pressures up to 15 kbar, we used a modified Merrill-Basset diamond-anvil cell [3,4]. The liquid immersion-technique [5] was used to load the cell with liquid nitrogen. A light-concentrating cone focused the light through the diamonds and sample and into a Ge:Cu photoconductor mounted directly behind the sample. We used the pressure dependence of the ALSb:Cs<sub>b</sub> LVM as a precise *in situ* calibration of the sample pressure [6].

### Wag modes.

The splittings of the wag harmonics are consistent with a complex which possesses  $C_{3v}$  symmetry. In the plane perpendicular to the  $[111]$  axis, the  $C_{3v}$  potential is given by [7,8]

$$V(x, y) = \frac{1}{2}k(x^2 + y^2) + B(xy^2 - x^3/3) + C(x^2 + y^2)^2 + \dots, \quad (1)$$

where  $x$  and  $y$  are parallel to the  $[1\bar{1}0]$  and  $[11\bar{2}]$  crystallographic axes, respectively. For simplicity, we have omitted the wag-stretch coupling terms. The anharmonic terms in Eq. 1 lift the degeneracy of the wavefunctions for  $N = n_x + n_y > 1$ . The predicted splittings are shown in Fig. 1. The dipole allowed transitions are the  $\Gamma_1 \rightarrow \Gamma_1$  and  $\Gamma_1 \rightarrow \Gamma_3$  transitions. The higher harmonics give rise to weaker peaks, since they require higher order anharmonic terms in Eq. (1). The theoretical wag frequencies are calculated with perturbation theory to second order for the cubic term and to first order for the quartic term. By adjusting the parameters  $k$ ,  $B$ , and  $C$ , a reasonable fit to experiment is obtained (Table I).

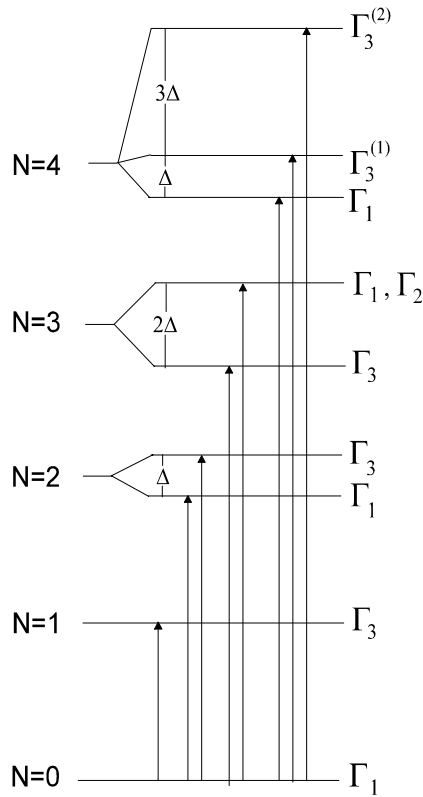


Figure 1. The splitting of the hydrogen/ deuterium wag modes in  $C_{3v}$  symmetry.

TABLE I. Theoretical and experimental values of Se-H and Se-D wag modes in AlSb.

$N$	Symm.	$0 \rightarrow N$ transition ( $\text{cm}^{-1}$ )			
		H (theory)	H (expt)	D (theory)	D (expt)
0	$\Gamma_1$				
1	$\Gamma_3$	342	ND	247	ND
2	$\Gamma_1$	666	666	484	478
2	$\Gamma_3$	689	692	496	497
3	$\Gamma_1$	1040	1032	748	742
3	$\Gamma_2$	1040	*	748	*
3	$\Gamma_3$	994	993	724	718
4	$\Gamma_1$	1304	1316	955	948
4	$\Gamma_3^{(1)}$	1327	1333	967	957
4	$\Gamma_3^{(2)}$	1396	ND	1002	ND
5	$\Gamma_1$	1665	ND	1212	ND
5	$\Gamma_2$	1665	*	1212	*
5	$\Gamma_3^{(1)}$	1629	ND	1193	ND
5	$\Gamma_3^{(2)}$	1735	ND	1247	ND

\*IR inactive

ND = not discovered

### Temperature dependence.

The temperature dependence of the Se-H and Se-D stretch modes is shown in Fig. 2. The linewidth broadening and shift to lower frequency with increasing temperature are seen in numerous semiconductor systems and are caused by an anharmonic interaction between the localized mode and acoustic phonons [9,10]. In our case, this temperature dependent broadening causes peaks 0 and 1 to overlap such that they are not resolved for temperatures greater than 40 K. For variable temperature measurements, therefore, we refer to the superposition of peaks 0 and 1 as “peak 1.”

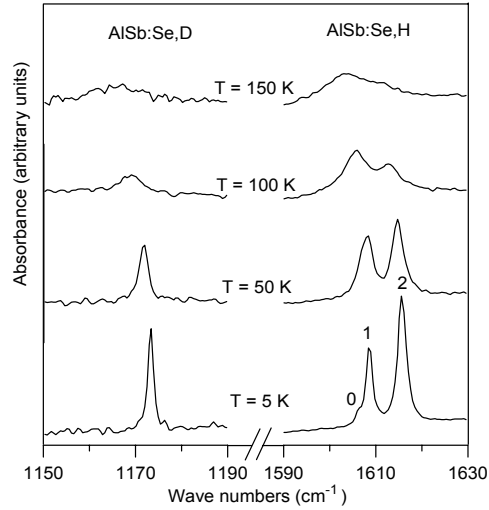


Figure 2. Temperature dependence of Se-D and Se-H stretch modes in AlSb.

To explain these observations, we propose a model in which the Se-H stretch LVM of energy  $\omega_{LVM}$  interacts with a nearly degenerate multi-phonon mode of energy  $\omega_{phonon}$ . The Hamiltonian is given by

$$H = H_{LVM} + H_{phon.} + H_{int.}, \quad (2)$$

where  $H_{LVM}$  and  $H_{phon.}$  are the Hamiltonians for the local and extended phonons, respectively, and  $H_{int.}$  is a weak interaction between these two systems. The phonon combinations that resonantly interact with the local mode are represented by a single energy  $\omega_{phonon}$ .

Treating  $H_{int.}$  as a small perturbation, we obtain the following matrix:

$$H = \begin{bmatrix} \omega_{LVM} & A \\ A & \omega_{phonon} \end{bmatrix}, \quad (3)$$

where  $A = \langle LVM | H_{int.} | phonon \rangle$ . The eigenvalues of this Hamiltonian are given by

$$\omega_{\pm} = \frac{1}{2} \left[ \omega_{LVM} + \omega_{phonon} \pm \sqrt{(\omega_{LVM} - \omega_{phonon})^2 + 4A^2} \right]. \quad (4)$$

The corresponding wavefunctions are given by

$$|\psi\rangle = a|LVM\rangle + b|\text{phonon}\rangle. \quad (5)$$

We refer to this linear combination of a local mode and a phonon as a *localon*. As explained below, the multi-phonon mode involves at least five phonons, and therefore has a negligible optical absorption cross section. The strength of the absorption peaks are determined by the LVM contribution to the wavefunction in Eq. (5), given by

$$|a|^2 = \frac{A^2}{(\omega_{LVM} - \omega_{\pm})^2 + A^2} \quad (6)$$

Experimentally,  $|a|^2$  represents the normalized area of peak 1:

$$|a|^2 = A_1/(A_1+A_2), \quad (7)$$

where  $A_1$  and  $A_2$  are the areas of peaks 1 and 2, respectively.

In our model, the temperature dependence of the unperturbed stretch mode is given by

$$\omega_{LVM} = 1612.7 - 0.034 U(T), \quad (8)$$

where  $U(T)$  is the mean vibrational energy of the lattice [9,10] in cal/mole and  $\omega_{LVM}$  is given in  $\text{cm}^{-1}$ . The frequency of the multi-phonon mode can be approximated by a constant independent of temperature,

$$\omega_{\text{phonon}} = 1611.2 \text{ cm}^{-1}, \quad (9)$$

where the parameters in Eqs. (8) and (9) were adjusted to fit the data. As the temperature increases, the area of peak 1 increases as it becomes more “LVM-like” (Fig. 3). Conversely, the area of peak 2 decreases as it becomes more “phonon-like.” Fig. 3 shows a comparison between the theoretical calculations and experimental results. Using a value of  $A = 3.45 \text{ cm}^{-1}$ , we can explain the temperature dependence of the peak positions [Fig. 3(a)] as well as the relative absorption strengths of the peaks [Fig. 3(b)].

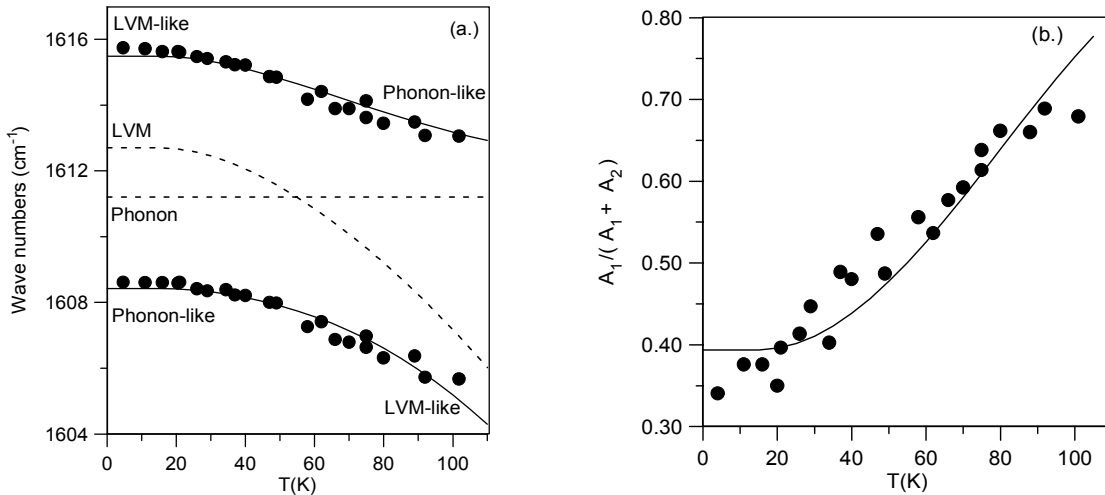


Figure 3. (a) Se-H stretch modes as a function of temperature. (b) Normalized area of Se-H peak 1 (lower-frequency peak). The solid lines are plots of the theoretical model.

This model also explains why we do not observe a splitting in the Se-D mode. The small interaction energy of  $A = 3.45 \text{ cm}^{-1}$  means that a local mode must lie within a few wavenumbers of the multi-phonon mode to show an appreciable splitting. The Se-D stretch mode at  $1173.4 \text{ cm}^{-1}$  is much too far below the multi-phonon mode at  $1611.4 \text{ cm}^{-1}$  to significantly interact. The same is true for the Te-H stretch mode at  $1599.0 \text{ cm}^{-1}$ , which also does not show a splitting.

### Pressure dependence.

To further probe the properties of this interaction, we used hydrostatic pressure to change the resonance conditions between the local and extended modes. Varying the pressure has an advantage over varying the temperature in that the lines do not broaden, so all three peaks are resolved. We find that the strength of peak 0, which is negligibly small at ambient pressure, increases rapidly at the expense of peaks 1 and 2. At pressures above 4.5 kbar, only peak 0 can be detected. The integrated absorption for all the peaks remains constant to within experimental error.

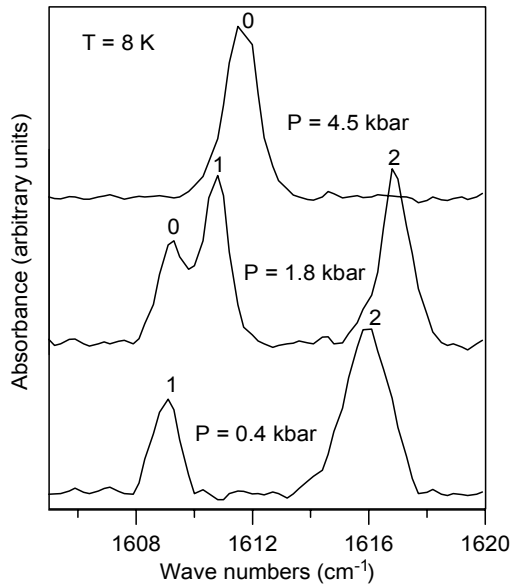


Figure 4. Se-H stretch mode peaks as a function of pressure.

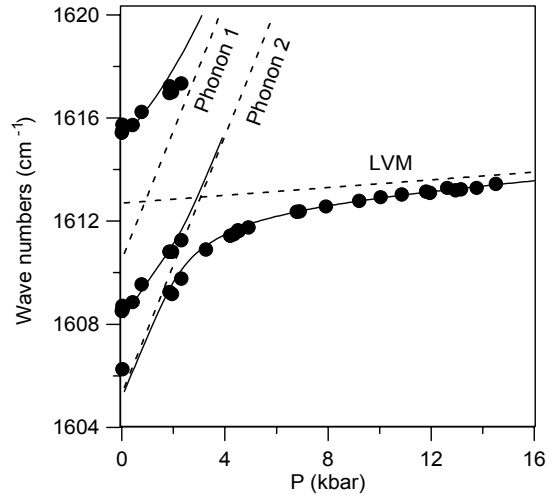


Figure 5. Se-H stretch mode peaks as a function of pressure. The dashed lines are the unperturbed LVM and multi-phonon modes and the solid lines are plots of the three-level theory.

To explain the pressure dependence of these peaks, we must consider the interaction of the LVM with two extended multi-phonon modes. The localon energies are given by

$$H = \begin{bmatrix} \omega_{LVM} & A & B \\ A & \omega_{phonon,1} & 0 \\ B & 0 & \omega_{phonon,2} \end{bmatrix}, \quad (10)$$

where  $A = \langle LVM | H_{int.} | phonon 1 \rangle$ ,  $B = \langle LVM | H_{int.} | phonon 2 \rangle$ , and for simplicity we have neglected the interaction between the multi-phonon modes. We use values of  $A = 3.45 \text{ cm}^{-1}$ , as before, and  $B = 1 \text{ cm}^{-1}$ . The pressure dependence of the LVM is given by

$$\omega_{LVM} = 1612.7 + 0.075 P, \quad (11)$$

where the zero pressure value of  $1612.7 \text{ cm}^{-1}$  is the same as that used in Eq. 8. To estimate the pressure dependence of the multi-phonon modes, we use the Grüneisen parameter for the zone-center LO phonon, yielding a pressure derivative given by  $d\omega/dP = 2.5 \text{ cm}^{-1}/\text{kbar}$ . The eigenvalues of the Hamiltonian (10) are calculated numerically. We obtain very good agreement between the model and experiment (Fig. 5).

We propose that the multi-phonon modes are different combinations of five phonons, since, e.g.,  $5 \times \omega_{\Gamma_0}(\Gamma) \sim 1610 \text{ cm}^{-1}$  is close to the observed frequencies. It has been suggested that the modes may be overtones of Se-H wag modes [11]. From perturbation theory, however, the  $N=5$ ,  $\Gamma_1$  wag mode has a predicted frequency of  $1665 \text{ cm}^{-1}$  (Table I), which is too far above the stretch mode ( $1610 \text{ cm}^{-1}$ ) to strongly interact. In addition, in  $C_{3v}$  symmetry there is only one  $N=5$ ,  $\Gamma_1$  wag mode, while we observe two “unknown” modes. However, we cannot exclude the possibility that the stretch mode resonantly interacts with a local vibrational mode of the Se-H complex that has not yet been discovered.

In conclusion, we have discovered evidence of a resonant interaction between local modes and phonons in AlSb. We propose that the Se-H stretch mode interacts with two different combinations of five phonons, resulting in anti-crossing between three distinct peaks. How a 5-phonon mode could have such a sharp resonance with the stretch mode, however, is an open question. One test of the 5-phonon model is to use temperature or pressure to tune a mode unrelated to the Se-H complex into resonance with the “unknown” mode. If the unknown mode is indeed a multi-phonon mode, then anti-crossing behavior should be observed.

We would like to thank L. Hsu for his assistance with the high-pressure work. This work was supported by in part by USNSF grant DMR-94 17763 and in part by the Director, Office of Energy Research, Office of Basic Energy Sciences, Materials Science Division of the U.S. Department of Energy under Contract No. DE-AC03-76SF00098.

## References.

1. J.-F. Zheng and M. Stavola, Phys. Rev. Lett. **76**, 1154 (1996).
2. M.D. McCluskey, E.E. Haller, W. Walukiewicz, and P. Becla, Phys. Rev. B **53**, 16297 (1996).
3. L. Merill and W.A. Bassett, Rev. Sci. Instr. **45**, 290 (1974).
4. E. Sterer, M.P. Pasternak, and R.D. Taylor, Rev. Sci. Instr. **61**, 1117 (1990).
5. D. Schiferl, D.T. Cromer, and R.L. Mills, High Temp. High Pressures **10**, 493 (1978).
6. M.D. McCluskey, L. Hsu, L. Wang, and E.E. Haller, Phys. Rev. B **54**, 8962 (1996).
7. R.C. Newman, Adv. Phys. **18**, 545 (1969).
8. M. Dean Sciacca, A.J. Mayur, N. Shin, I. Miotkowski, A.K. Ramdas, and S. Rodriguez, Phys. Rev. B **51**, 6971 (1995).
9. R.J. Elliot, W. Hayes, G.D. Jones, H.F. MacDonald, and C.T. Sennet, Proc. R. Soc. Lond. **A289** 1 (1965).
10. M.D. McCluskey, E.E. Haller, J. Walker, and N.M. Johnson, Phys. Rev. B **52**, 11859 (1995).
11. B. Clerjaud and C. Van de Walle, private communication.